AD-A051 523 NAVY ELECTRONICS LAB SAN DIEGO CALIF F/G 17/1
DIMUS MARK I RECEIVING SYSTEM FOR LORAD MARK III.(U)
MAY 61 C J KRIEGER
UNCLASSIFIED NEL-1046 NL

1 OF 1
AD A051523

END
DATE FILMED
4-78
DDC

RESEARCH AND DEVELOPMENT REPORT
REPORT 1046
29 MAY 1961

NEL/Report 1046

689B 9/4/61

MOST Project-3

(12) 42 p.

(14) NEL-1046

(6) DIMUS Mark I Receiving System for Lorad Mark III (C)

(10) C. J. KRIEGER

689B

ORIGINAL CONTAINS COLOR PLATES: ALL DDC REPRODUCTIONS WILL BE IN BLACK AND WHITE

U. S. NAVY ELECTRONICS LABORATORY, SAN DIEGO, CALIFORNIA
A BUREAU OF SHIPS LABORATORY

THE PROBLEM

Develop an active sonar (Lorad) for the detection of submarines in deep water at ranges of 100 miles or more, and in shallow water in excess of 10 miles. Specifically, design, install, and evaluate an improved receiving system for Lorad Mark III.

RESULTS

A receiving system designated DIMUS (DIgital MUltibeam Steering) was developed. Tests showed that this system, using five samples per cycle, has satisfactory beam-forming capability and its bearing precision is equal to that obtainable with other methods, such as delay lines.

RECOMMENDATION

Use DIMUS in place of delay lines in future Lorad design, provided that the simpler, passive phase compensator cannot be employed.

ADMINISTRATIVE INFORMATION

This report covers work from approximately January 1960 to March 1961 by members of the Special Research Division and others under AS 02101-5, S-F001 03 02 (NEL E1-3) as a portion of the general Lorad program and was approved for publication 29 May 1961.

The author expresses appreciation to the Marine Physical Laboratory, University of California, for the design and procurement of shift-register boards and various components and for advice in the assembly and operation of

DIMUS; to J. Wong, L. D. Morgan, J. A. Thomson, and R. J. Vachon, who participated in the design, assembly, laboratory evaluation, and sea trials; and to R. P. Kempff, who analyzed the records.

Appreciation is also expressed for the cooperation of the officers and men of USS BAYA (AGSS 318) and USS REXBURG (EPCER 855) during the sea tests of DIMUS.

CONTENTS

ILLUSTRATIONS

ILLUSTRATIONS (Continued)

TABLES

SYMBOLS

n = Element number from 1 to 60
d = Spacing between elements
θ = Angle of arrival measured from array normal
θ_c = Angle of compensation
ΔT = Time delay
c = Sound velocity
B_w = Number of bits assigned to water path
B_s = Number of bits in shift register
k = Integer
A = Positive-going point on square wave
C = Array center
R = Amplitude of beam output
P = Polarity of 1500-c/s square wave
B_n = Bit difference relative to array center
F = Clock frequency
N = Number of shift register bits

INTRODUCTION

Beam formation in the past has usually been accomplished by means of delay lines. In a steered sonar system, different sets of adjacent hydrophones are, in turn, connected to the same delay line, thus producing maximum response throughout 360° in azimuth, but in only one direction at a time. Hence, the manual search rate is rather low. If a mechanical scanning switch is employed, time-sharing and loss of information result.

In a multibeam sonar, a delay line can be used for each desired beam, and each hydrophone output is connected to the proper tap on each delay line. Since all outputs are available to the operator simultaneously there is no search-rate problem, and all available information is fully used. An example is an installation made for Lorad aboard USS BAYA.[1]

Mechanical scanning switches introduce problems of switching noise and maintenance, while batteries of delay lines take up scarce shipboard floor space.

Another approach to multibeam formation is phase compensation, which involves the use of transformers with pairs of secondary windings equaling the number of beams to be formed. Such a phase compensator was developed and installed for Lorad station-keeping.[2] Phase compensators are primarily intended for single-frequency or narrow-band operation but their applicability to broad-band operation has also been demonstrated.[3]

---

[1] Navy Electronics Laboratory Report 968, Lorad Mark III Receiving System-Bearing Calibration and Self-Noise, by C. J. Krieger, CONFIDENTIAL, 11 May 1960

[2] Navy Electronics Laboratory Report 757, Simultaneous Multibeam Phase Compensation, Part VI: Phase Compensator for the Lorad Station-Keeping Receiver System, by C. J. Krieger and R. P. Kempff, CONFIDENTIAL, 7 May 1957

[3] Navy Electronics Laboratory Report 1009, Simultaneous Multibeam Phase Compensation: Part X. Broadband Application by F. R. Abbott. 8 December 1960

A third approach to multibeam formation is DIMUS (DIgital MUltibeam Steering).[4] The clipped signals are fed into shift registers, and advanced by means of clock pulses. By connecting the proper taps on the shift registers, any number of desired beams can be obtained simultaneously (fig. 1).

The study to be reported here includes the design of DIMUS, laboratory evaluation and sea trials, and a comparison of its performance with that of delay lines.

---

[4]Anderson, V. C., "Digital Array Phasing," Acoustical Society of America. Journal, v. 32, p. 867-870, July 1960

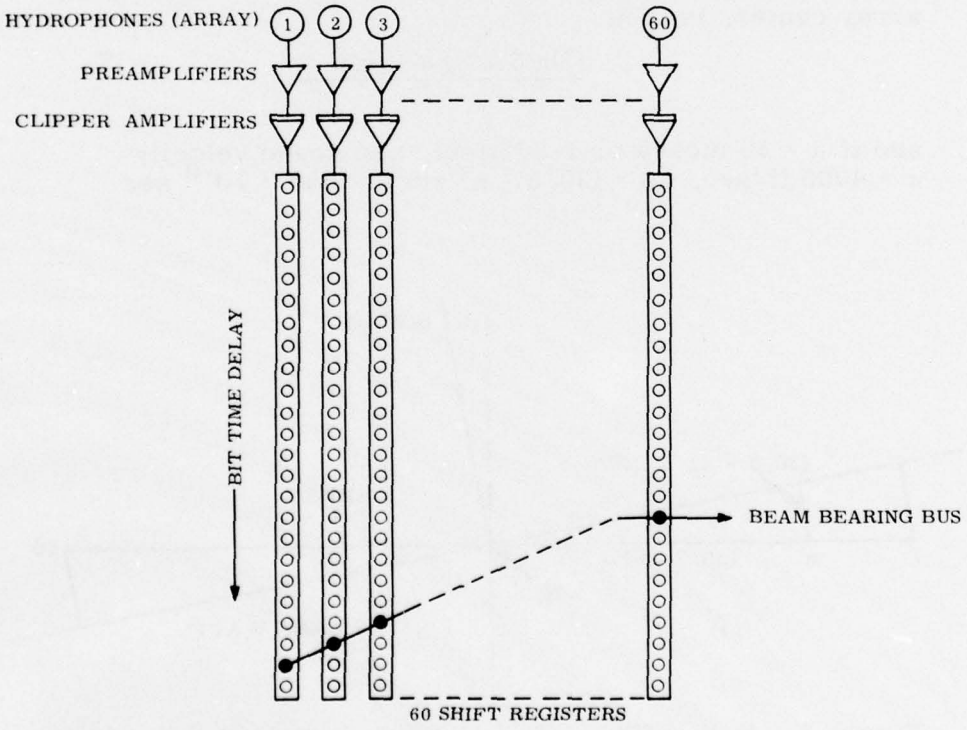

Figure 1. Schematic diagram of Lorad DIMUS.

DETAILS OF DIMUS DESIGN

EXPRESSIONS FOR THE DELAYS IN THE WATER PATH AND THE SHIFT REGISTER

Delay in the Water Path Referred to the Array Center

It may be seen from figure 2 that the path difference at the n^{th} element, referred to the array center, is $(30.5 - n)\, d \cdot \sin \theta$, where

- n is the element number from 1 to 60
- d the spacing between elements
- θ the angle of arrival measured from the array normal

The time delay ΔT at the n^{th} element, still referred to the array center, is then

$$\frac{(30.5 - n)\, d \cdot \sin \theta}{c}$$

and if d = 20 inches or 1-2/3 feet, and sound velocity c = 4900 ft/sec, $\Delta T = (30.5 - n) \sin \theta \cdot 340 \cdot 10^{-6}$ sec.

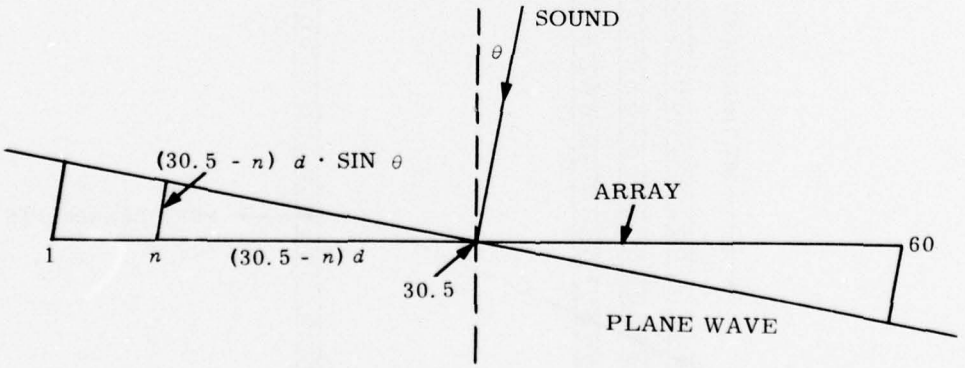

Figure 2. Path difference of plane wave referred to array center at nth element of a linear array.

Let us now assume a signal frequency of 1500 c/s and assume that the information is advanced along the shift register at the rate of 7500 clock pulses per second; then the corresponding number of bits in the water path is:

$$(30.5 - n) \sin\theta \cdot 340 \cdot 7500 \cdot 10^{-6} = 2.55 \sin\theta\,(30.5 - n)$$

where one bit is equivalent to one flip-flop in the shift register. To eliminate negative delays, which cannot be realized with this method, we add the maximum number of bits expected at either array end for $\theta = \pm 60°$, namely

$$29.5 \cdot \sin 60° \cdot 340 \cdot 7500 \cdot 10^{-6} = 65.2$$

Hence, the number of bits B assigned to the water path is

$$B_w = 65.2 + 2.55 \cdot \sin\theta \cdot (30.5 - n)$$

Delay in the Shift Register Referred to the Array Center

In order to refer the arrival time from all directions to the array center, and since the maximum angles of compensation are $\pm 60°$, the number of bits in the shift register B_s are chosen so that $B_w + B_s \approx 130.4$ when $\theta = \theta_c$ for any hydrophone n. (θ_c is the angle of compensation.) This demands that

$$B_s = 65.2 + 2.55 \cdot \sin\theta_c \cdot (n - 30.5)$$

One stage (bit) was added at the input of each shift register in order to provide a tap for zero delay.

Combined Delay in the Water Path and in the Shift Register

The total number of bits is then

$$B_w + B_s = 130.4 + 2.55 (\sin\theta_c - \sin\theta) \cdot (n - 30.5)$$

In choosing shift register taps, fractions are rounded up or down, and the actual number of taps may differ from the calculated number by ± 1.

DIRECTIVITY PATTERN WITH SINGLE FREQUENCY SIGNAL

Maximum output is obtained if all shift register taps used in beam formation are in the same state, say "1," at one time. A given tap delivers information either "1" or "0," 7500 times per second. If the shift register inputs are 1500-c/s square waves, then either three "1's" or two "0's," or the reverse, will be delivered at any tap during one cycle, i.e., in 1/1500 second. The amplitude variation in time of one beam, holding θ_c and θ constant, can be obtained analytically by adding the outputs of all taps involved in forming this beam, at selected instants during one cycle.

There is a simple way of finding the elements n where the difference of bits $B_w + B_s$ relative to the array center has reached $\pm 1/2$, $\pm 3/2$, $\pm 5/2$, etc., and where, therefore, a whole bit must be added or subtracted.

Set

$$2.55\,(\sin\theta_c - \sin\theta)\,(n - 30.5) = \pm 1/2,\ \pm 3/2, \ldots \frac{2k-1}{2};\quad k = 1.2\ldots$$

Solving,

$$n = 30.5 \pm \frac{2k-1}{5.10(\sin\theta_c - \sin\theta)}$$

For $\theta = \theta_c$, no values of n between 1 and 60 exist, and therefore all taps deliver the same information.

Now let

$$\theta_c = 60^\circ \text{ and } \theta = 54^\circ, \text{ with } \sin\theta_c - \sin\theta = .05701,$$

$$n = 30.5 \pm \frac{1}{.2910} = 30.5 \pm 3.45 \text{ or } 27.05 \text{ and } 33.95$$

and

$$n = 30.5 \pm \frac{3}{.2910} = 20.2 \text{ and } 40.7, \text{ and so forth.}$$

If we refer all bits to the array center, then the distribution of bits shown in figure 3 results.

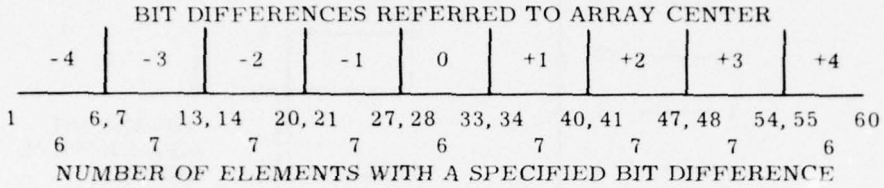

Figure 3. Distribution of bit differences referred to array center, for $\theta_c = 60°$ and $\theta = 54°$.

The algebraic sign in the left half of the array is taken as negative since at $\theta = 54°$ the water path there is shorter then at $\theta_c = 60°$. These bit differences, it should be realized, are caused by the fact that the plane wave arrives from a direction other than the direction of compensation, and that the plane wave is sampled five times per cycle. This results in either two "1" states and three "0" states in one cycle of the signal frequency, or the reverse.

The total output, at any time, will depend on the relative position of the advancing square wave which carries the information. Let us examine the situation when the positive-going point *A* on the square wave has just passed the array center *C*, where the bit difference is zero (fig. 4). At this moment there will be 33 "1's"; two-tenths of a cycle later, in the dotted position, there will be 32 "1's." Continuing this process we arrive at the following amplitude variation:

Phase of square wave at *C* counted from positive-going point *A* in fractions of signal period	Amplitude of beam output (*R*)
0	33
0.2	32
0.4	33
0.6	41
0.8	41
1.0	33

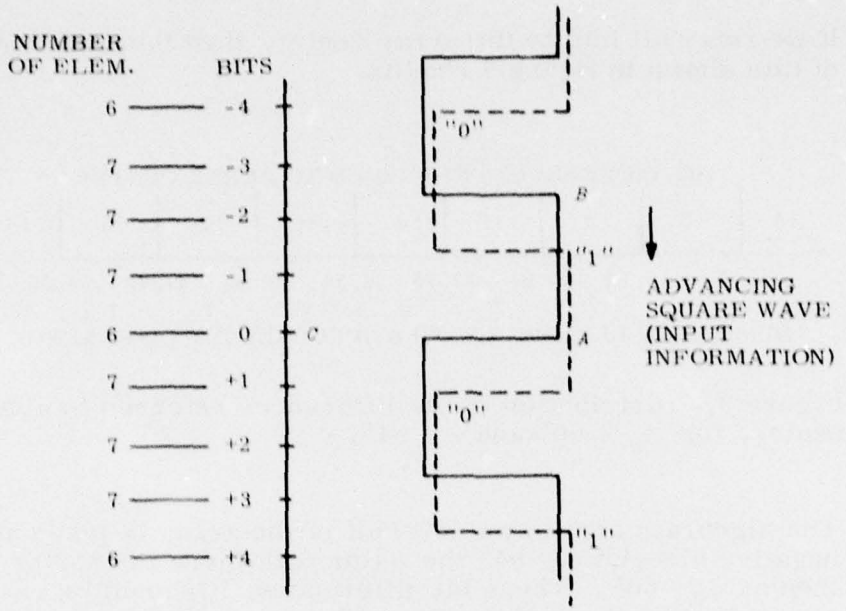

Figure 4. Output amplitude determination with nomographic method, for $\theta_c = 60°$ and $\theta = 54°$.

Nomographic Method

These numbers can be obtained easily by drawing the square wave on transparent paper, advancing it two-tenths of a cycle at a time, and adding the number of "1" outputs. An even more convenient method is to cut windows in a piece of opaque paper to correspond to the "1" states. Only these states would be counted, since the "0" states are covered. Plotting the response R against the phases at which the samples were taken and repeating the procedure at two

angles of compensation and several angles of arrival, the results shown in figures 5 and 6 were obtained. The resulting curves contain the 1500-c/s signal frequency in which we have the greatest interest, in addition to a constant and some higher frequencies. The former can be isolated by means of a band-pass filter or found, approximately at least, by a graphical analysis as shown in the figures.

The maximum amplitudes of the signal are a measure of the response of the system to a signal arriving from the chosen direction, i.e., the directivity function. Two of these have been plotted in figures 7 and 8; the values are shown in solid lines. There is good agreement with the values obtained by the usual analog method, employing delay lines. The corresponding values are plotted in dotted lines.

If ten samples instead of five were taken in one cycle, the clock frequency and the number of bits per element would be doubled for the same bearing angle coverage. The resulting responses are shown in figures 9 and 10; the corresponding points are shown as dashed lines in figures 7 and 8. The results do not differ appreciably from those obtained by taking five samples; the latter choice is therefore justified.

Analytical Method

A method has been devised which can be adapted for use with a computer, if desired. In brief, first the bit difference relative to the array center is calculated for the taps which are used in beam formation. Then the upward crossing of the square wave representing the information is lined up with the array center, and the polarity of the square wave is noted at all taps involved in beam formation. The sum of all positive polarities is a measure of the response. Next, the square wave is advanced one bit, or $2\pi/5$ radians in phase at a time, and the process is repeated until five samples have been obtained for each direction of compensation and angle of arrival.

Bit Differences Relative to Array Center

From an earlier equation we have

$$B_w + B_s = 130.4 + 2.55 (\sin \theta_c - \sin \theta) (n - 30.5)$$

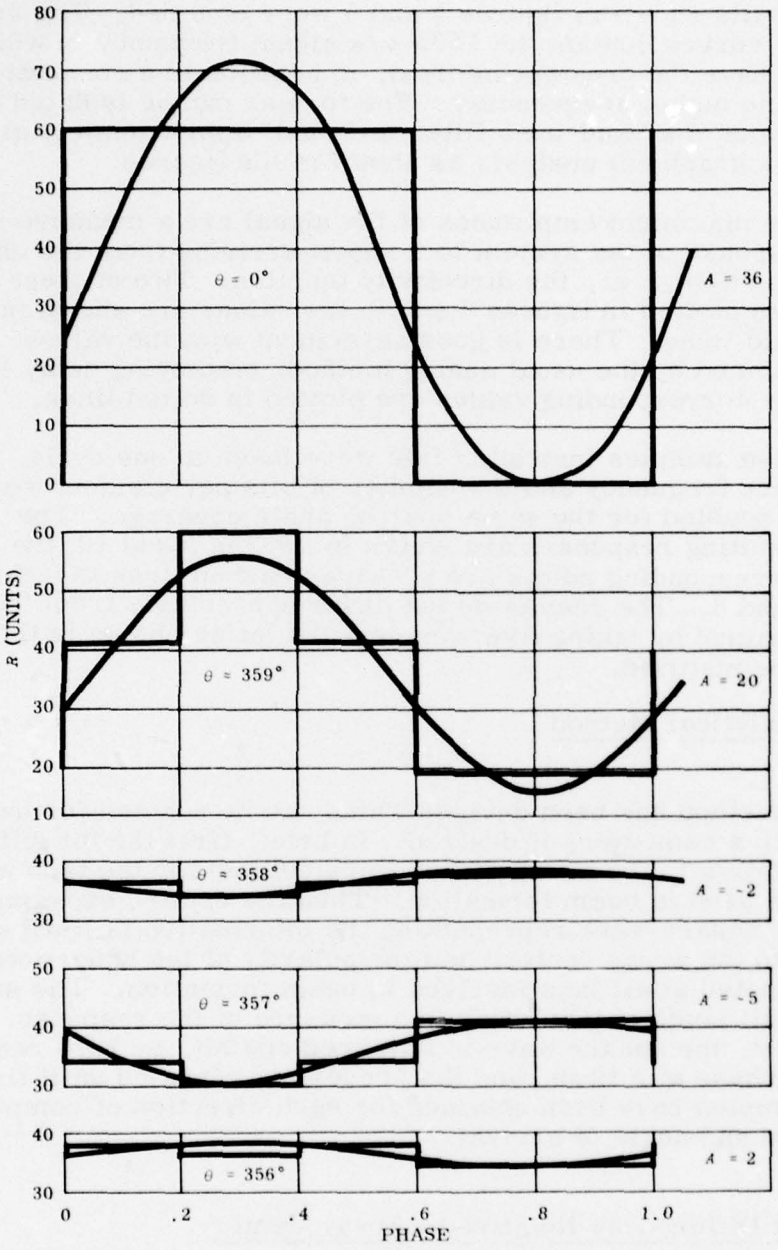

Figure 5. Amplitude variation for $\theta_c = 0°$ and various values of θ; five samples per period; 1500-c/s signal frequency.

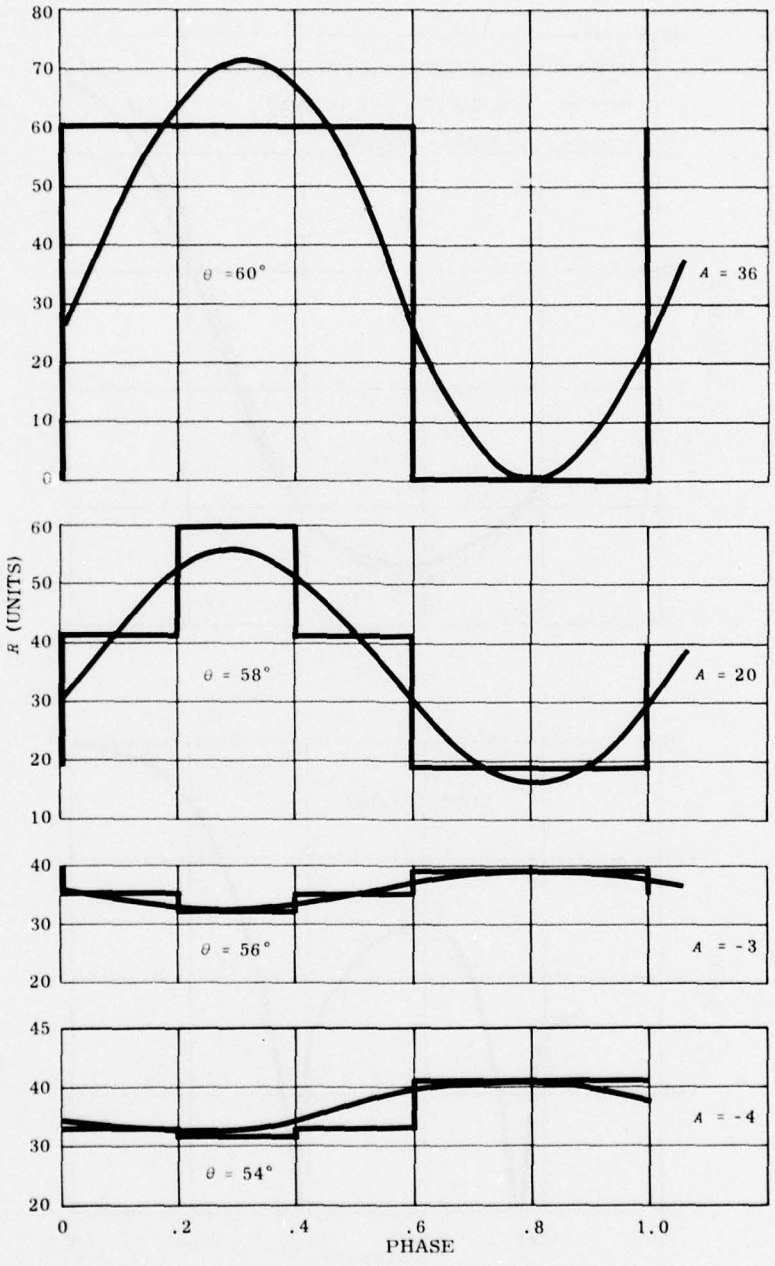

Figure 6. Amplitude variation for $\theta_c = 60°$ and various values of θ; five samples per period; 1500-c/s signal frequency.

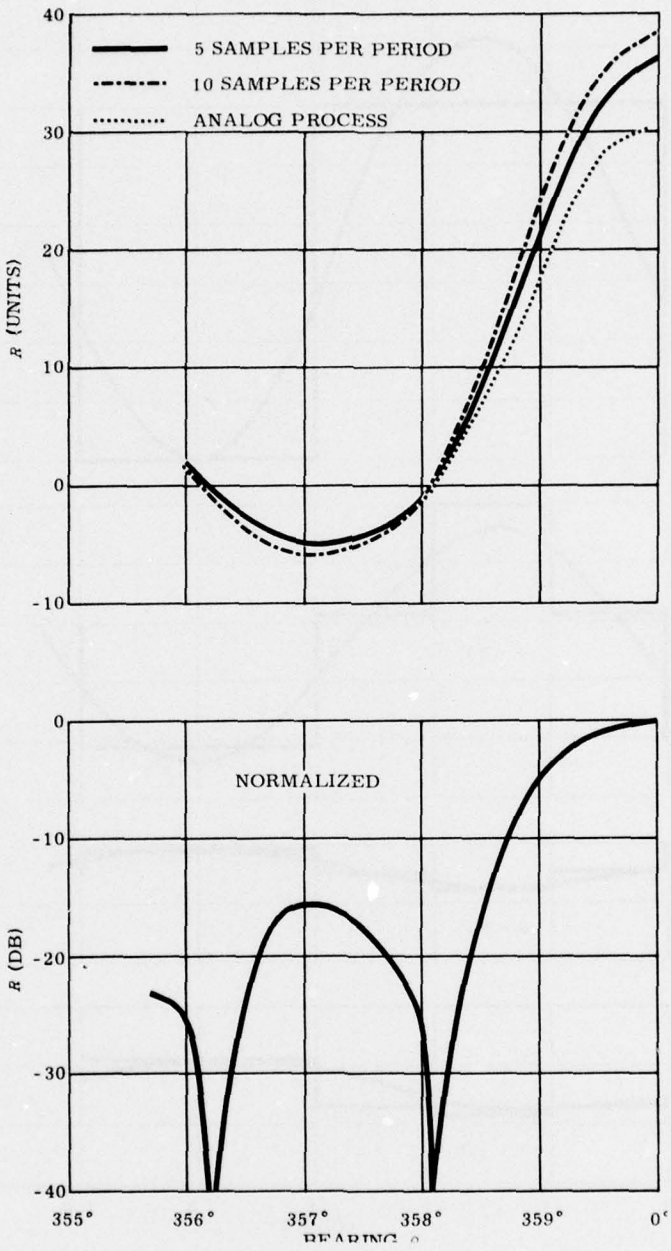

Figure 7. DIMUS directivity pattern as a function of θ; $\theta_c = 0°$; five and ten samples per period, also analog process; 1500-c/s signal frequency.

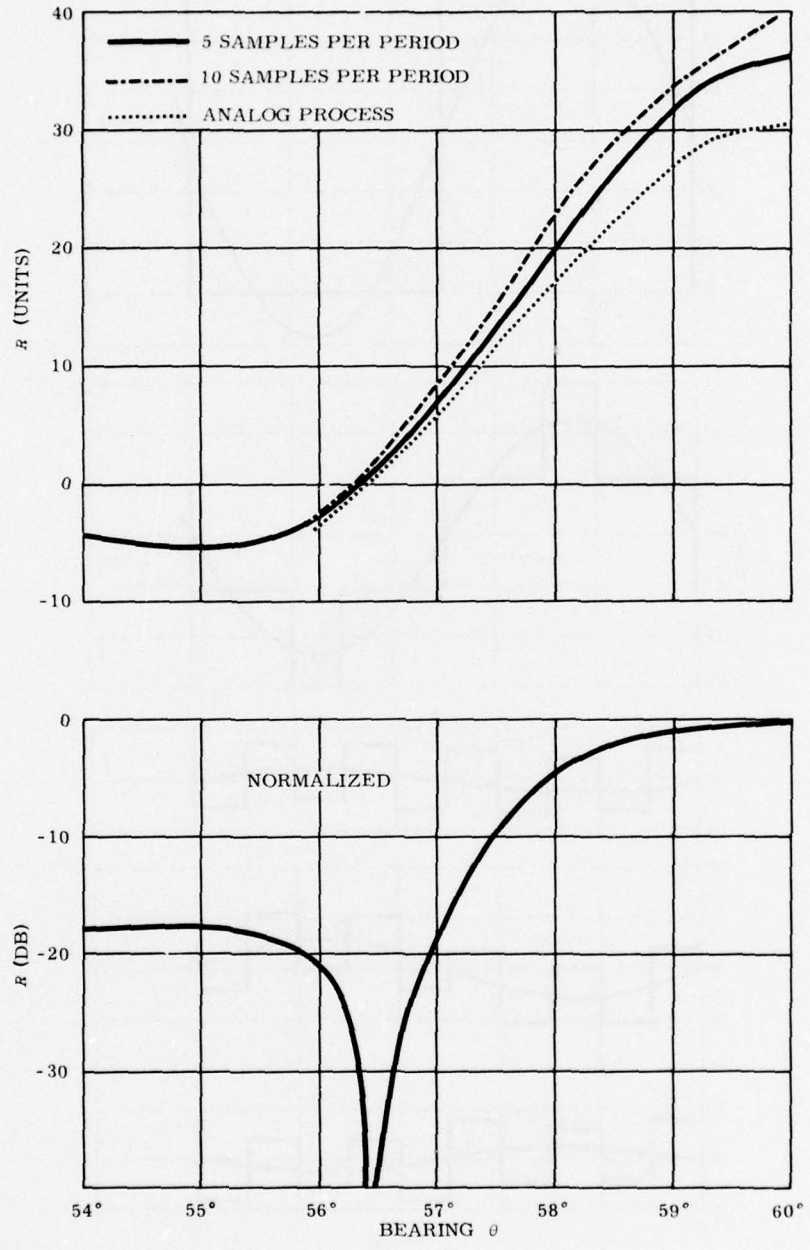

Figure 8. DIMUS directivity pattern as a function of θ; $\theta_c = 60°$; five and ten samples per period, also analog process; 1500-c/s signal frequency.

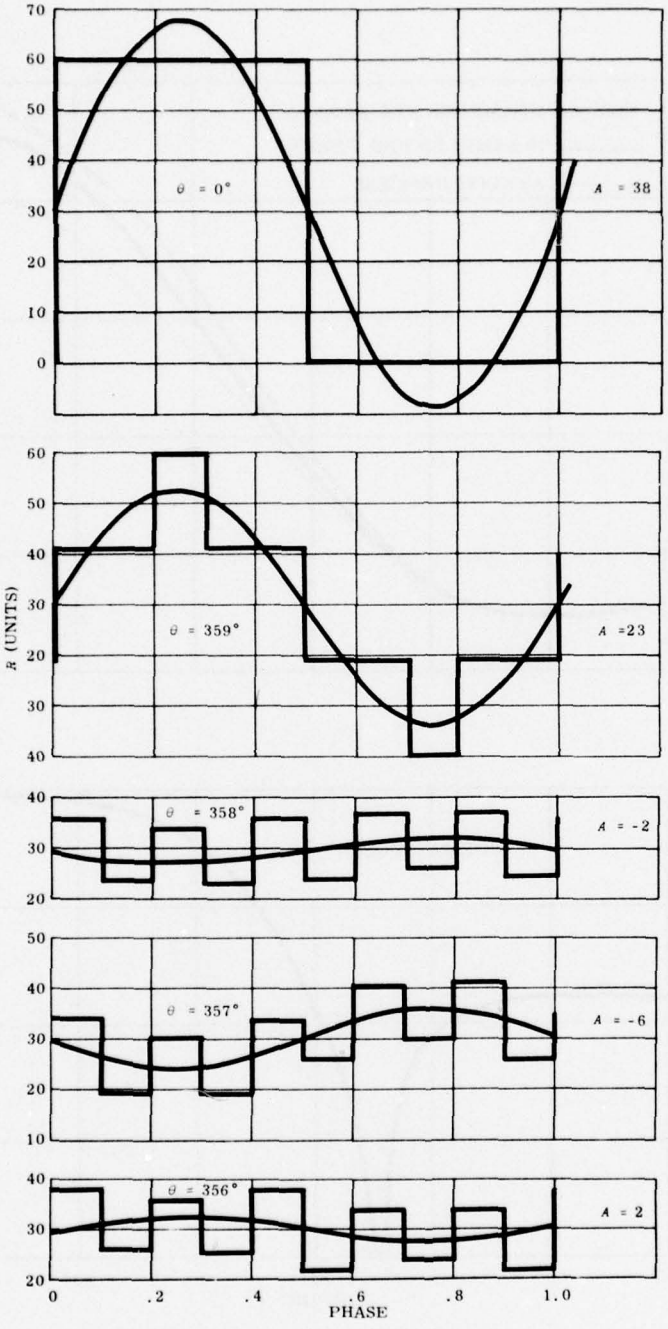

Figure 9. Amplitude variation for $\theta_c = 0°$ and various values of θ; ten samples per period; 1500-c/s signal frequency.

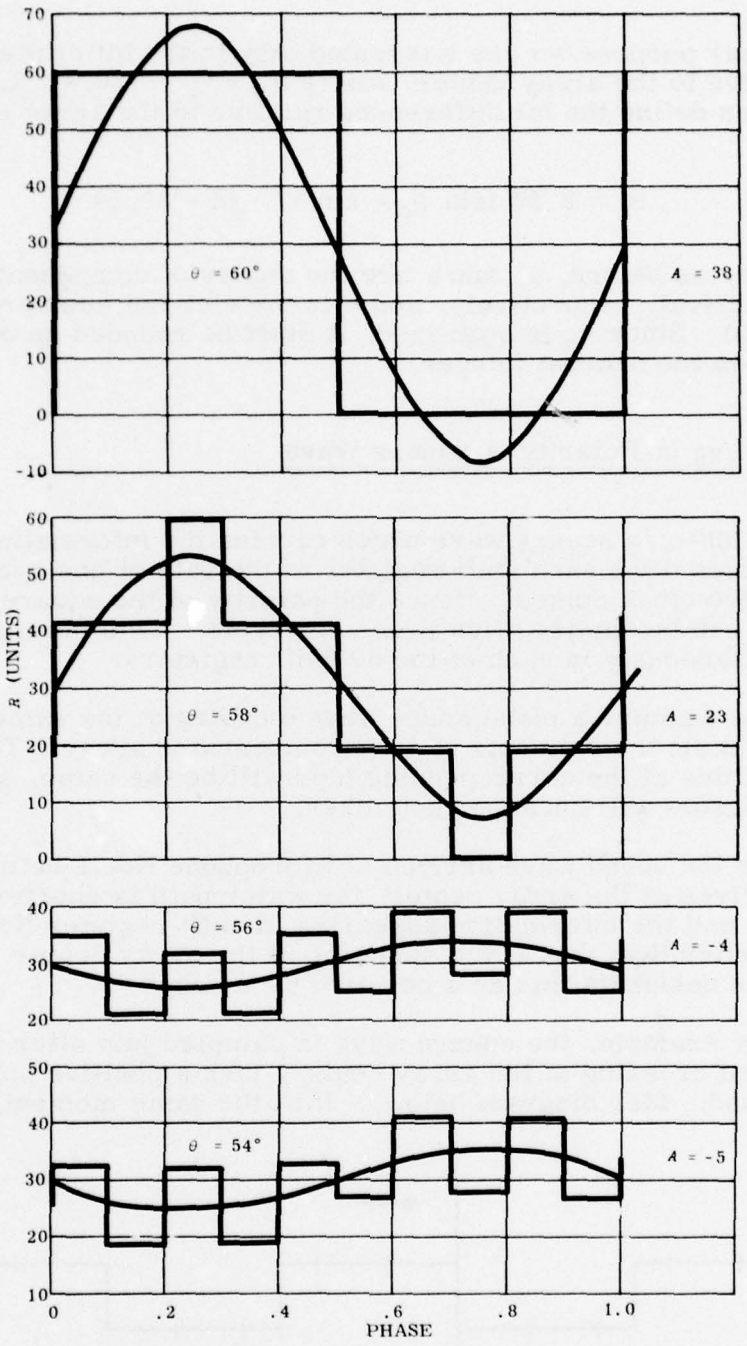

Figure 10. Amplitude variation for $\theta_c = 60°$ and various values of θ; ten samples per period; 1500-c/s signal frequency.

For our purpose we are interested only in the bit differences relative to the array center, where $B_w + B_s = 130.4$. Let us then define the bit differences relative to the array center as

$$B_n = 2.55 (\sin \theta_c - \sin \theta) \cdot (n - 30.5)$$

where, as before, θ_c and θ are the angles of compensation and arrival, respectively, and n is the element number from 1 to 60. Since B_n is quantized, it must be rounded up or down to the nearest integer.

Sampling of Polarity of Square Wave

The 1500-c/s square wave which carries the information advances down each shift register at the rate of one cycle per five clock pulses. Hence the polarity of the square wave can be sampled five times per cycle. This occurs simultaneously in each of the 60 shift registers.

Let us examine a plane sound wave arriving at the same time at all the elements of an uncompensated array. The polarities at the corresponding taps will be the same, and the signals will enhance each other.

If now the sound wave arrives at hydrophone No. 1 before it arrives at the array center, the water path is shorter there and the information appearing in shift register No. 1 is earlier than that at the same tap at the array center. Let us designate this as a negative bit number.

If, for example, the square wave is sampled just after the upward crossing at the array center, then a positive polarity is found. (See diagram below.) If, at the same moment, it

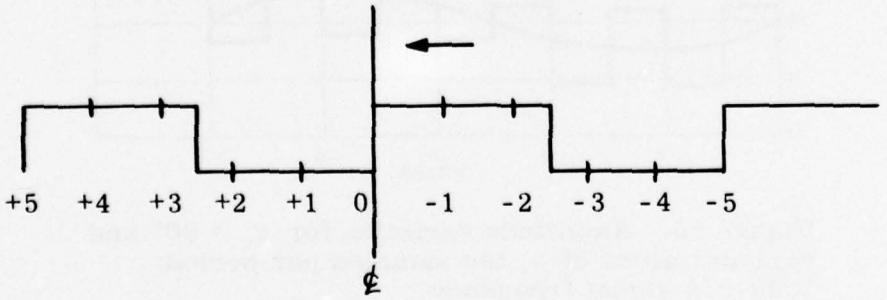

is sampled at hydrophone No. 1 where the bit difference may be -4, then the polarity would be 0. At hydrophone No. 60, on the other hand, where the bit difference may be +4, the polarity would be 1. The sum of the last two outputs would thus be 1. The 58 other outputs would have to be added to obtain the total array response.

We can summarize our findings in the form of a table:

+5	+4	+3	+2	+1	0	-1	-2	-3	-4	-5
1	1	1	0	0	1	1	1	0	0	1

One-fifth of a cycle, or one pulse, later, more recent information appears at all taps. This can be expressed by stating that the bit differences B_n have increased by -1 (or decreased by 1). It can also be interpreted as a motion of the square wave to the left, or down the shift register:

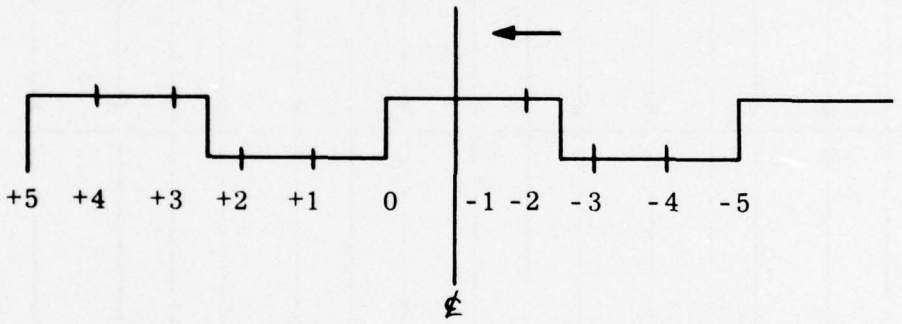

The System Response

Proceeding as before, the responses in various directions are found.

Table 1 illustrates the procedure, and results for $\theta_c = 60°$ and $\theta = 54°$ are shown. The column headings are

n = element number
B_n = bit difference relative to array center
B_c = bit number at array center
P = polarity of 1500 c/s square wave

TABLE 1. SYSTEM RESPONSE R FOR $\theta_c = 60°$, $\theta = 54°$

5 SAMPLES PER CYCLE;

CLIPPED 1500 C/S SINE WAVE

	$B_c = 0$		$B_c = -1$		$B_c = -2$		$B_c = -3$		$B_c = -4$	
n	B_n	P	B_n	P	B_n	P	B_n	P	B_n	P
1	-4	0	-5	1	-1	1	-2	1	-3	0
2										
3										
4										
5										
6										
7	-3	0	-4	0	-5	1	-1	1	-2	1
8										
9										
10										
11										
12										
13										
14	-2	1	-3	0	-4	0	-5	1	-1	1
15										
16										
17										
18										
19										
20										
21	-1	1	-2	1	-3	0	-4	0	-5	1
22										
23										
24										
25										
26										
27										
28	0	1	-1	1	-2	1	-3	0	-4	0
29										
30										
31										
32										
33										

TABLE 1. (CONT'D)

	$B_c = 0$		$B_c = -1$		$B_c = -2$		$B_c = -3$		$B_c = -4$	
n	B_n	P	B_n	P	B_n	P	B_n	P	B_n	P
34	+1	0	0	-1	-1	1	-2	1	-3	0
35	↓	↓	↓	↓	↓	↓	↓	↓	↓	↓
36	↓	↓	↓	↓	↓	↓	↓	↓	↓	↓
37	↓	↓	↓	↓	↓	↓	↓	↓	↓	↓
38	↓	↓	↓	↓	↓	↓	↓	↓	↓	↓
39	↓	↓	↓	↓	↓	↓	↓	↓	↓	↓
40	↓	↓	↓	↓	↓	↓	↓	↓	↓	↓
41	+2	0	+1	0	0	1	-1	1	-2	1
42	↓	↓	↓	↓	↓	↓	↓	↓	↓	↓
43	↓	↓	↓	↓	↓	↓	↓	↓	↓	↓
44	↓	↓	↓	↓	↓	↓	↓	↓	↓	↓
45	↓	↓	↓	↓	↓	↓	↓	↓	↓	↓
46	↓	↓	↓	↓	↓	↓	↓	↓	↓	↓
47	↓	↓	↓	↓	↓	↓	↓	↓	↓	↓
48	+3	1	+2	0	+1	0	0	1	-1	1
49	↓	↓	↓	↓	↓	↓	↓	↓	↓	↓
50	↓	↓	↓	↓	↓	↓	↓	↓	↓	↓
51	↓	↓	↓	↓	↓	↓	↓	↓	↓	↓
52	↓	↓	↓	↓	↓	↓	↓	↓	↓	↓
53	↓	↓	↓	↓	↓	↓	↓	↓	↓	↓
54	↓	↓	↓	↓	↓	↓	↓	↓	↓	↓
55	+4	1	+3	1	+2	0	+1	0	0	1
56	↓	↓	↓	↓	↓	↓	↓	↓	↓	↓
57	↓	↓	↓	↓	↓	↓	↓	↓	↓	↓
58	↓	↓	↓	↓	↓	↓	↓	↓	↓	↓
59	↓	↓	↓	↓	↓	↓	↓	↓	↓	↓
60	↓	↓	↓	↓	↓	↓	↓	↓	↓	↓
$R = \sum_{1}^{60} B_n$	33		32		33		41		41	

Here,

$B_n = 0.1455\ (n - 30.5)$ and the system response is $R = \sum_{n=1}^{60} B_n$.

The system response R ranges from 32 to 41 and is, as might be expected, identical with the results obtained with the nomographic method (fig. 6).

In general, the nomographic method will be preferable if only a small number of points on the directivity pattern are wanted; on the other hand, the analytical method when adapted for computer use would be chosen if a large number of points are wanted.

In an actual system, it may be expected that fluctuations in the relative phases at the array elements, finite rise time, and other departures from the underlying assumptions, will result in a statistical rather than strictly algebraic summing of the sixty tap outputs.

DIRECTIVITY PATTERN WITH BROADBAND SIGNAL

The preceding discussion has shown that the directivity pattern obtained from a single frequency, using shift registers, is practically identical with that obtained with delay lines. If another single frequency differing from the design frequency is used, then the number of samples taken per cycle will also differ, but the previous discussion and figures 9 and 10 indicate that the direction of maximum response is not altered. It is further concluded that this statement holds also for a broadband signal, which is composed of numerous single frequencies. However, changes in minor lobes and nulls must be expected.

To illustrate the results that may be expected, a signal composed of three frequencies, 1450, 1500, and 1550 c/s, and a sampling frequency of 7500 c/s were chosen, and the resulting directivity pattern was obtained with the nomographic window method. Table 2 shows the responses at different directions of arrival for the three frequencies. The amplitudes R shown in the last column were obtained from graphs or by inspection of the tabulated values; the response of 36 at 60°, however, was obtained by a Fourier analysis. The responses at the three frequencies were

TABLE 2. SYSTEM RESPONSE R FOR $\theta_c = 60°$, DIMUS CLOCK FREQUENCY 7500 C/S. SIGNAL FREQUENCIES 1450, 1500, AND 1550 C/S

	PHASE									
θ	-.8	-.6	-.4	-.2	0	+.2	+.4	+.6	+.8	R
					1450 C/S					
60°	60	60	00	0	60	60	60	0	0	+36*
58°	60	41	19	19	41	60	41	19	0	+30
57°	44	37	31	31	37	44	37	23	16	+14
56°25'	36	36	36	36	36	36	36	24	24	+6
56°	32	35	38	39	35	32	31	29	28	-5.5
55°	26	34	43	43	34	25	26	34	35	-9
54°	26	33	41	41	33	26	25	34	34	-8
					1500 C/S					
60°	60	60	0	0	60	60	60	0	0	+36*
58°	60	41	19	19	41	60	41	19	19	+20.5
57°	44	37	31	31	37	44	37	31	31	+6.5
56°25'	36	36	36	36	36	36	36	36	36	0
56°	32	35	39	39	35	32	35	39	39	-3.5
55°	26	34	43	43	34	26	34	43	43	-8.5
54°	32	33	41	41	33	32	33	41	41	-4.5
					1550 C/S					
60°	60	60	0	0	60	60	60	0	0	+36*
58°	41	41	19	19	41	60	41	19	19	+20.5
57°	34	29	31	31	37	44	37	31	31	+7.5
56°25'	24	24	36	36	36	36	36	36	36	-6
56°	21	25	35	39	35	32	35	39	39	-9
55°	18	25	35	42	34	26	34	43	43	-12.5
54°	25	26	34	35	33	32	33	41	41	-8

*By Fourier analysis.

combined assuming a random phase relationship; the resulting directivity pattern obtained is shown in table 3. The pattern is presented in figure 11 as a broken curve. As predicted, maximum response is still at 60°; the minor lobe is about -11 db and the depth of the first null is about -17 db.

TABLE 3. DIRECTIVITY PATTERN R FOR $\theta_c = 60°$, DIMUS CLOCK FREQUENCY 7500 C/S.

SIGNAL FREQUENCIES 1450, 1500, 1550 C/S

θ	R^2			ΣR^2	R		Rel. db
	1450 C/S	1500 C/S	1550 C/S		$\sqrt{\Sigma R^2}$	db	
60°	1300	1300	1300	3900	62.5	35.9	0
58°	900	420	420	1740	41.8	32.4	-3.5
57°	196	42	56	294	17.2	24.7	-11.2
56°25'	36	0	36	72	8.5	18.6	-17.3
56°	30	12	81	123	11.1	20.9	-15.0
55°	81	72	156	309	17.5	24.9	-11.0
54°	64	20	64	148	12.2	21.7	-14.2

For comparison purposes, the directivity pattern resulting from a delay line was then computed from the expression

$$\frac{R}{R_o} = \frac{\sin 60 \frac{\pi d}{\lambda} (\sin \theta_c - \sin \theta)}{\sin \frac{\pi d}{\lambda} (\sin \theta_c - \sin \theta)}$$

where $\theta_c = 60°$ and $d = 5/3$ foot. The same three frequencies and random phase relationship were used, as above. The resulting directivity pattern is shown in figure 11 as a solid curve. The general character of the two patterns is quite

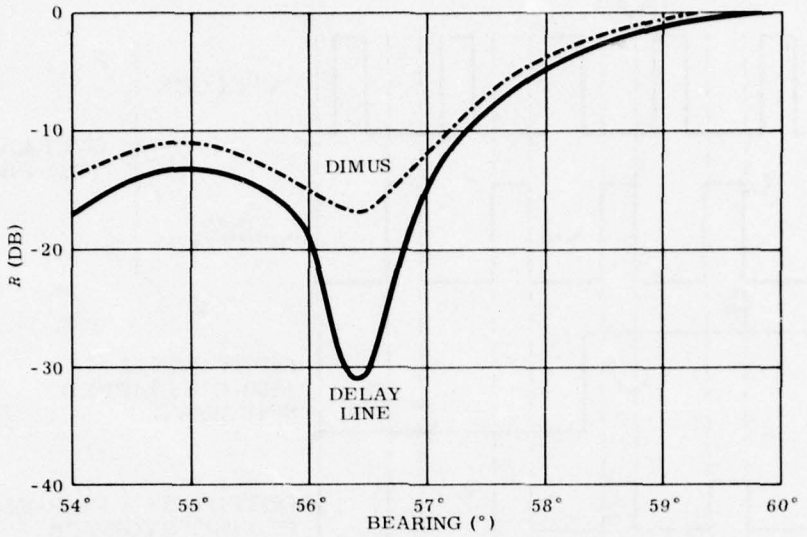

Figure 11. Comparative directivity patterns for DIMUS and delay line as a function of θ; $\theta_c = 60°$; signal frequencies 1450, 1500, and 1550 c/s.

similar, but the delay line pattern has a lower minor lobe level and a deeper null. It should be borne in mind that in the DIMUS analysis a signal duration of less than 2 cycles was used; for longer signals, a time dependency of the pattern may be expected, but an averaged pattern will result.

SHIFT REGISTERS AND BEARING BUS ASSEMBLY

No attempts are made in this report to present the details of equipment design. While the preceding discussion is based on well known conventional shift registers, it applies equally well to the shift register actually used in this application. The operation of these flip-flops is unique because information is advanced by means of an overlapping two-phase clock which turns the collector supply on and off. This results in a flip-flop output which is the amplitude-modulated clock pulse sequence (fig. 12).

Although the waveforms at the shift register taps are different from those in the conventional circuits, the methods of calculating directivity patterns given earlier are still applicable.

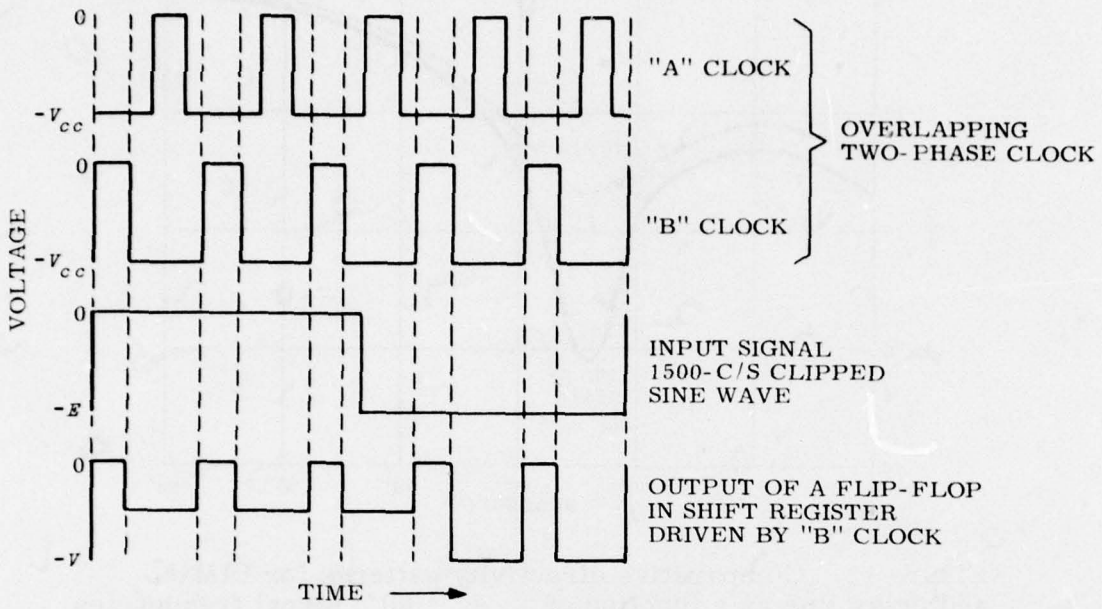

Figure 12. Waveform of flip-flop using overlapping two-phase clock.

Through the cooperation of the Marine Physical Laboratory of the University of California, the required shift-register boards were procured. The taps to be connected for the formation of the 121 beams were determined by the methods described previously (p. 9) and tabulated. The wiring of the supporting rails was accomplished by an outside contractor; final assembly was performed at NEL. Figure 13 shows the DIMUS cabinet installed aboard USS BAYA.

Detailed wiring diagrams are not included in this report, but are available upon request. Address U. S. Navy Electronics Laboratory, San Diego 52, California, attention Code 2320.

Figure 13A. DIMUS cabinet installation aboard USS BAYA, with front panel in place.

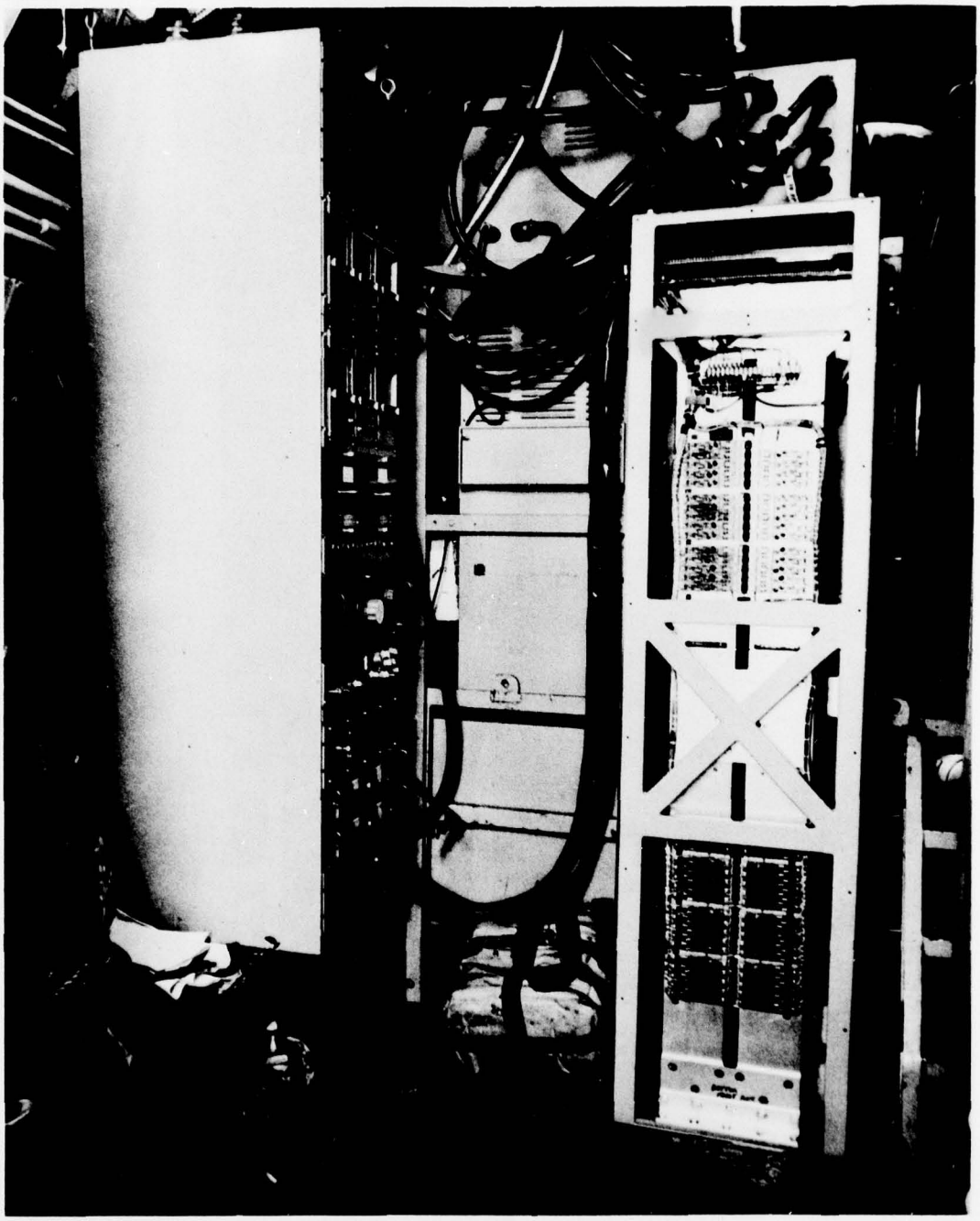

Figure 13B. DIMUS cabinet installation aboard USS BAYA, with front panel removed.

LABORATORY EVALUATION

RESPONSE TO SIMULATED PLANE WAVES

Upon completion of the 121-beam DIMUS matrix, input signals simulating arriving plane waves were applied to the inputs, after clipping. The matrix output was passed through a 1250- to 1750-c/s band-pass filter. Three test results are described here:

A. An input signal of 1500 c/s was applied in phase to 56 operative channels (of the 60 design channels). This test simulates a target at relative bearing 000°.

Figure 14 shows the response of the 121 output channels or bearing buses, numbered from 1 to 121 to correspond to relative bearings from 300° to 060°. It should be emphasized that this is not a directivity pattern; rather it depicts the simultaneous outputs of the 121 channels, in response to a source at 000°. Maximum response does occur in channel 61, i.e., at relative bearing 000°. The response of the adjacent channels is about 4 db lower, as expected from their beam width of about 2°; beam separation is 1°. All other channels respond substantially less, in keeping with the design objectives.

B. This test was the same as test A, except that the input signal was random noise in a 1200- to 1700-c/s band, in phase.

Figure 15 shows that the response at the bearing of the source (000°) and of the adjacent channels is quite similar to that produced in test A. The response of the remaining channels is more uniform and lower, without marked spikes. This statistical smoothing effect is to be expected with broad-band inputs.

C. An input signal of random noise in a 1200- to 1700-c/s band was applied to channels 1 to 50 with required phase differences, by means of a delay line, to simulate a plane wave arriving from relative bearing 311.5°. (This bearing resulted from the use of an available delay line designed for different element spacing.)

Figure 16 shows that maximum responses occur at relative bearings 311° and 312°; hence the relative bearing of the source is 311.5°, as expected. The responses of the remaining channels are uniform and low, as in test B.

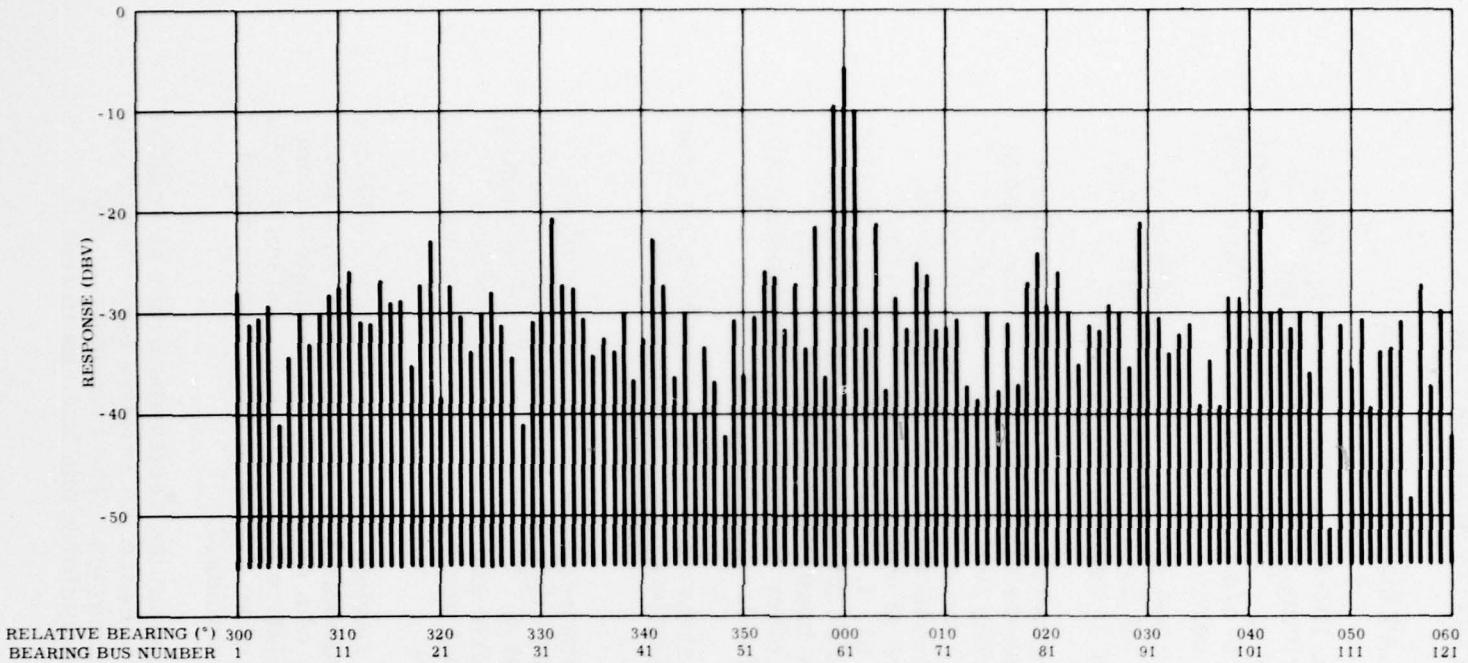

Figure 14. Response of DIMUS matrix to simulated plane wave from 000°. Input, 1500 c/s, clipped; amplitude, 4.5 v. Output, emitter follower, filtered. 56 active elements.

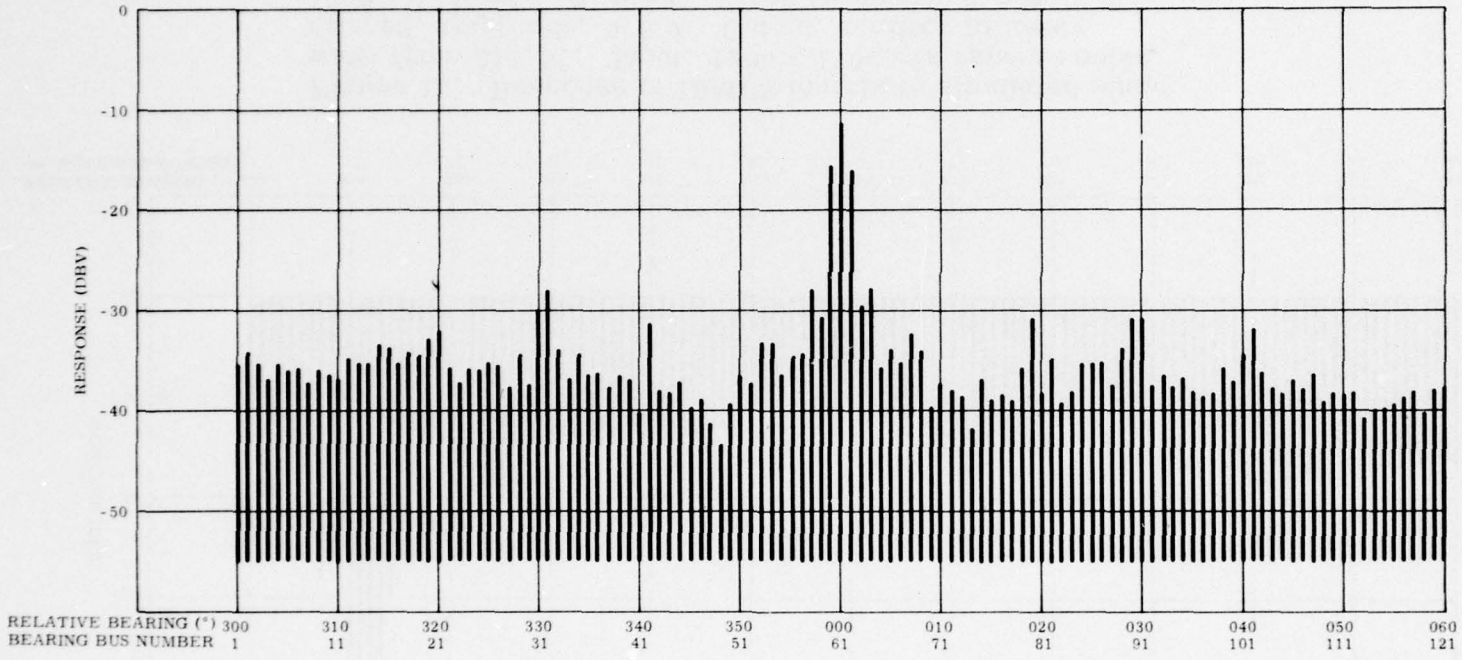

Figure 15. Response of DIMUS matrix to simulated plane wave from 000°. Input, 1200 - 1700 c/s random noise, clipped; amplitude, 4.5 v. Output, emitter follower, 1250 - 1750 c/s, filtered. 56 active elements.

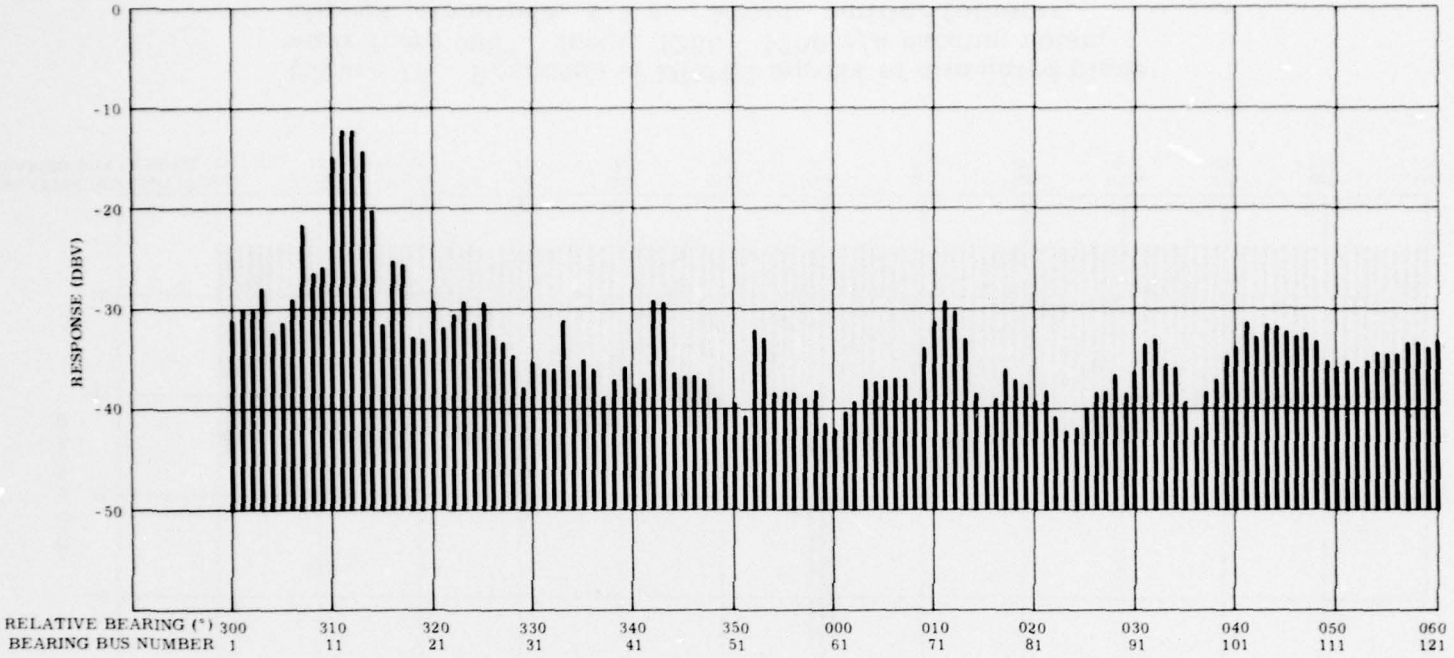

Figure 16. Response of DIMUS matrix to simulated plane wave from 311.5°. Input, 1200 - 1700 c/s random noise, clipped; amplitude, 4.5 v. Output, emitter follower, 1250 - 1750 c/s, filtered. Clock frequency 7.5 kc/s ± 1 c/s.

A clock frequency of 7.5 kc/s ± 1 c/s was maintained by monitoring with an electronic counter, since the indicated bearing is a function of the clock frequency.

EFFECT OF CLOCK FREQUENCY ON INDICATED BEARING

The number of shift register bits N needed between adjacent elements is $\frac{d \sin \theta}{c} F$ where F is the clock frequency, and d, c, θ have their usual meaning. Consider a plane wave arriving from 300° at the extreme elements, numbers 1 and 60 of the array. The difference in bits required is $N = \frac{59\ d}{c} \sin \theta_c \cdot F$. If F is increased to F', then the information in channel 1 has advanced through $N' = \frac{59\ d}{c} \sin \theta \cdot F'$ units by the time the same plane wave arrives at element 60. Hence phasing is accomplished at a bearing bus bar which was designed for a bearing θ_c at the normal clock frequency F. Thus,

$$\frac{59\ d}{c} \sin \theta \cdot F' = \frac{59\ d}{c} \sin \theta_c \cdot F$$

and the indicated bearing θ_c is defined by

$$\sin \theta_c = \sin \theta \cdot \frac{F'}{F}$$

i.e., farther from the array normal than the correct bearing θ.

The following values were obtained experimentally when the source was simulated at $\theta = 311.5$ with a design clock frequency $F = 7.5$ kc/s:

F' (kc/s)	Measured θ_c	Calculated θ_c
7.4	312.5	312.4
7.45	312	311.9
7.5	311.5	311.5
7.6	310.5	310.6

The agreement is very satisfactory. Clearly, it is essential to use a very stable and controllable clock frequency.

At the same time, the relation between clock frequency and indicated bearing can be utilized for beam steering.

From

$$N = \frac{59\ d}{c} \cdot \sin \theta_c \cdot F$$

we find

$$d\theta_c = - \tan \theta_c \cdot \frac{dF}{F}$$

provided that c is constant.

Hence a small change in clock frequency will result in a predictable change in the indicated bearing.

CLOCK FREQUENCIES FOR DIFFERENT VELOCITIES OF SOUND

It can also be shown that the indicated bearing θ_c will change if the sound velocity c differs from the design value while the design clock frequency F is constant. In order to maintain a correct θ_c, F must be changed. From the equation

$$N = \frac{59\ d}{c} \sin \theta_c \cdot F$$

it follows that

$$F' = \frac{c'F}{c}$$

where F' and c' are the new values of clock frequency and sound velocity, respectively, and F and c are the corresponding design values.

BEARING CALIBRATIONS

Bearing calibrations were made at sea on 26 and 27 January 1961. USS REXBURG (EPCER 855), while lying to in 700 fathoms, lowered a 24-inch-diameter barium titanate transducer 50 feet and transmitted 0.5-second pulses spaced 2.0 seconds at 1500 c/s, or random noise in a band from 1250 c/s to 1750 c/s.[1] USS BAYA (AGSS 318), on which a 100-foot linear array[1] and the DIMUS system were installed described tight counterclockwise circles at periscope depth. The average range was approximately 2000 yards; range measurements were made three times during each run. Periscope bearings of the source were obtained at 1° intervals and marked on two paper recorders, together with the outputs of ten bearing channels (also called beams). Consequently, both the acoustical and periscope bearings were known simultaneously.

Five runs were made with the DIMUS equipment, and 500 bearing readings were taken, i.e., an average of about four for each of the 121 beams.

Also, three runs were made with the delay lines.[1] In one run, the outputs of the DIMUS and the delay lines were recorded simultaneously, for a direct comparison.

The results of the five DIMUS runs are shown in figure 17; each run is represented by symbols and colors.

The periscope readings have not been smoothed, although their irregular spacing in time suggests a fair amount of scatter. A smoothing procedure would involve an unjustified expenditure of time and effort.

The acoustical bearings have been corrected for the two known effects, namely parallax and velocity of sound. The array is located about 100 feet forward of the periscope and the parallax is of the order of about 0.5°, depending on both range and bearing. A sound velocity of 4932 ft/sec was obtained from bathythermograms taken several times during the test. Corrections to the design velocity of 4900 ft/sec are of about the same magnitude as the parallax corrections, but have the opposite algebraic sign.

Figure 17 shows that the errors are independent of bearing, and that the majority carry a negative algebraic sign. The extremes are +1.4° and -1.4°.

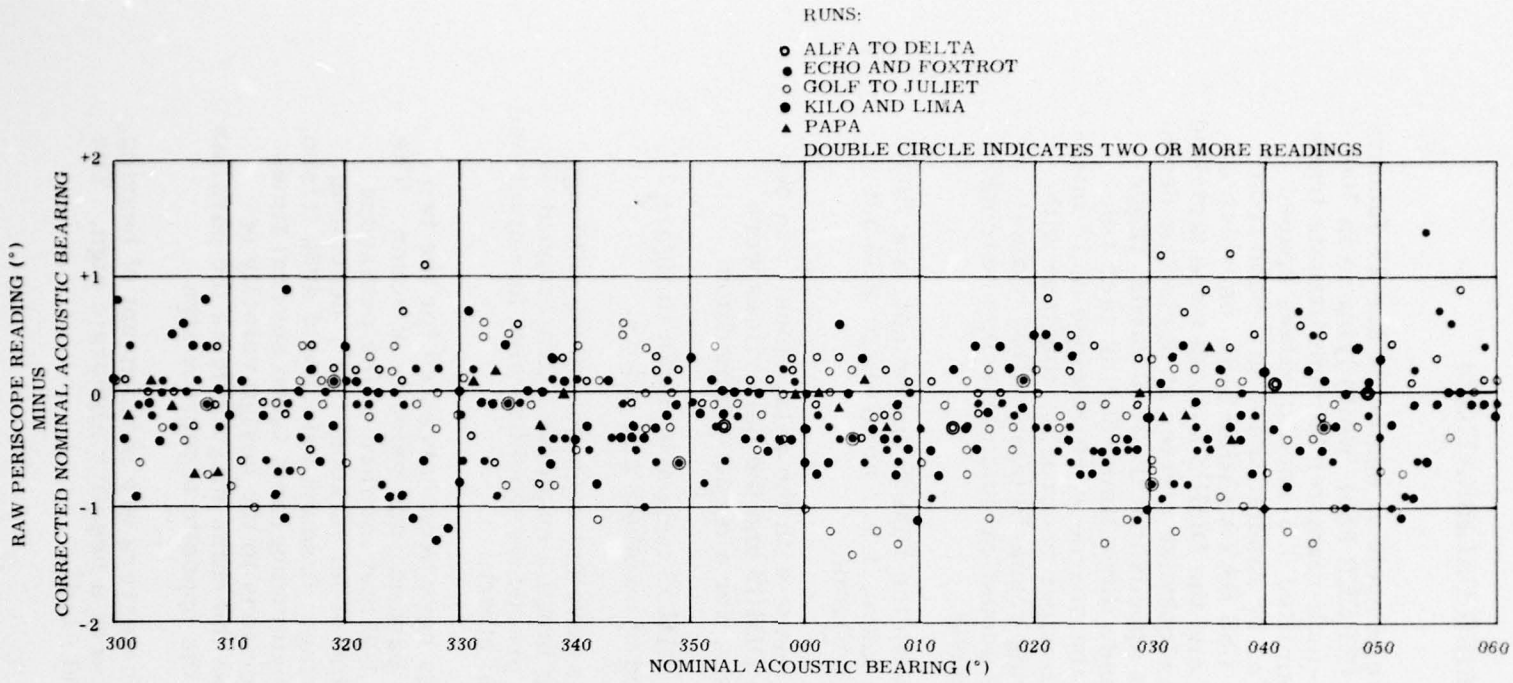

Figure 17. Results of sea tests using Lorad Mark III receiving system with DIMUS Mark I, showing raw periscope reading minus corrected nominal acoustic bearing.

The distribution of the errors is shown in figure 18. As stated before, corrections for parallax and velocity of sound had been made. The mean $\bar{x} = 0.18°$ indicates that periscope readings could be increased by +0.18° or 11' to make the periscope zero point agree with the average acoustical zero point. Conversely, all acoustical bearings could be decreased by the same amount. The standard deviation is ±0.45°; this includes errors in reading periscope bearing, and in locating maximum response on the paper records; also any equipment errors in design and construction, including the effect of quantization of the signal input. It is not possible to separate human errors and equipment errors, but examination of the records indicates that human errors are almost certainly the larger.

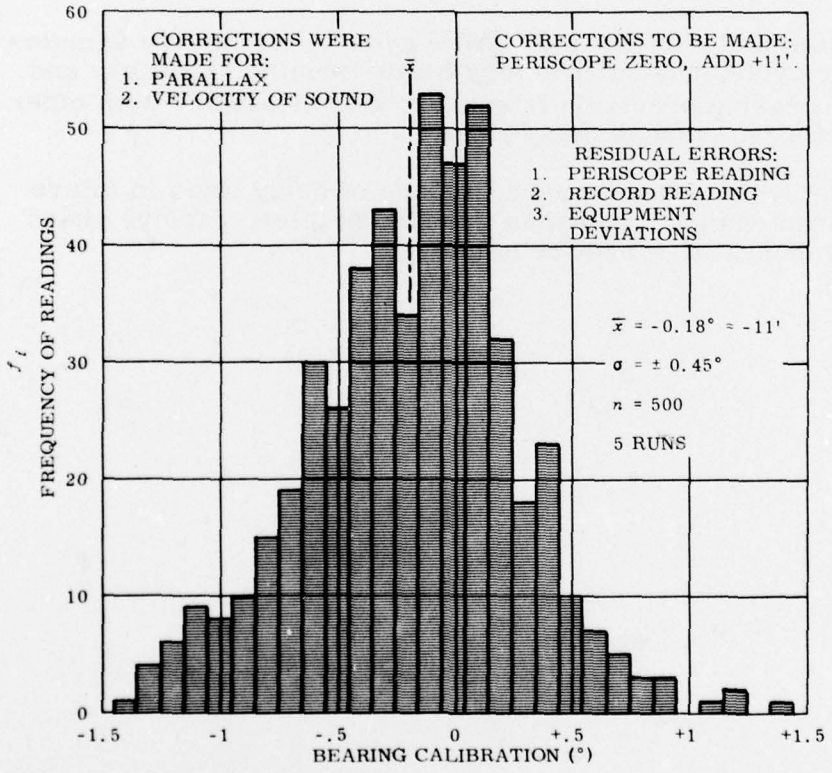

Figure 18. Distribution of errors in figure 17. Corrections were made for parallax and velocity of sound.

The inherent bearing precision of DIMUS is believed to be greater than the results of this test would indicate. However, a test procedure eliminating or greatly reducing human judgment would be required to demonstrate this.

The delay line tests which were made at the same time as the DIMUS tests gave practically the same results, namely the same zero point correction and standard deviation.

Reliability of this DIMUS system has hinged largely on the reliability of the shift-register boards in which, up to the present, a fair number of failures have occurred, almost solely due to poor solder connections. A preventive maintenance program is planned.

CONCLUSIONS

Tests indicate that the DIMUS system, using five samples per cycle, has satisfactory beam-forming capability and its bearing precision is equal to that obtainable with other methods, such as delay lines.

The system may be used in place of delay lines in future Lorad designs, provided that the simpler, passive phase compensator cannot be employed.

Navy Electronics Laboratory
Report 1046

DIMUS MARK I RECEIVING SYSTEM FOR LORAD MARK III (C), by C. J. Krieger. 40p., 29 May 1961.
CONFIDENTIAL

A receiving system designated DIMUS (DIgital MUltibeam Steering) was developed for the Lorad Mark III. Tests show that this system, using five samples per cycle, has satisfactory beam-forming capability and its bearing precision is equal to that obtained with other methods, such as delay lines.

1. DIMUS
2. Lorad Mk III - Equipment

I. Krieger, C. J.

AS 02101-5
S-F001 03 02 (NEL E1-3)

This card is CONFIDENTIAL

UNCLASSIFIED

Navy Electronics Laboratory
Report 1046

DIMUS MARK I RECEIVING SYSTEM FOR LORAD MARK III (C), by C. J. Krieger. 40p., 29 May 1961.
CONFIDENTIAL

A receiving system designated DIMUS (DIgital MUltibeam Steering) was developed for the Lorad Mark III. Tests show that this system, using five samples per cycle, has satisfactory beam-forming capability and its bearing precision is equal to that obtained with other methods, such as delay lines.

1. DIMUS
2. Lorad Mk III - Equipment

I. Krieger, C. J.

AS 02101-5
S-F001 03 02 (NEL E1-3)

This card is CONFIDENTIAL

UNCLASSIFIED

Navy Electronics Laboratory
Report 1046

DIMUS MARK I RECEIVING SYSTEM FOR LORAD MARK III (C), by C. J. Krieger. 40p., 29 May 1961.
CONFIDENTIAL

A receiving system designated DIMUS (DIgital MUltibeam Steering) was developed for the Lorad Mark III. Tests show that this system, using five samples per cycle, has satisfactory beam-forming capability and its bearing precision is equal to that obtained with other methods, such as delay lines.

1. DIMUS
2. Lorad Mk III - Equipment

I. Krieger, C. J.

AS 02101-5
S-F001 03 02 (NEL E1-3)

This card is CONFIDENTIAL

UNCLASSIFIED

Navy Electronics Laboratory
Report 1046

DIMUS MARK I RECEIVING SYSTEM FOR LORAD MARK III (C), by C. J. Krieger. 40p., 29 May 1961.
CONFIDENTIAL

A receiving system designated DIMUS (DIgital MUltibeam Steering) was developed for the Lorad Mark III. Tests show that this system, using five samples per cycle, has satisfactory beam-forming capability and its bearing precision is equal to that obtained with other methods, such as delay lines.

1. DIMUS
2. Lorad Mk III - Equipment

I. Krieger, C. J.

AS 02101-5
S-F001 03 02 (NEL E1-3)

This card is CONFIDENTIAL

UNCLASSIFIED

INITIAL DISTRIBUTION LIST

Bureau of Ships
  Code 335 Code 421
  Code 670 Code 672E
  Code 673 Code 688 (2)
  Code 320 Code 689B1
  Code 315 Code 689C1
  Code 331 Code 321A
  Code 360
Bureau of Naval Weapons
  DLI-3 DLI-31 (2)
  RUDC-11 RUDC-2 (2)
Chief of Naval Personnel
  Technical Library
Chief of Naval Operations
  Op-07T Op-73 (2)
  Op-03EG Op-07T23
Chief of Naval Research
  Code 411 Code 461
  Code 466 Code 492
  Code 493 Code 455
Commander in Chief, Lant Flt
Commander in Chief, Pac Flt
Commander Operational Test & Evaluation Force, Lant
Operational Test & Evaluation Force, Pacific Projects Staff
Commander Destroyer Force, Lant Flt
Commander Submarine Force, Pac Flt
Commander Submarine Force, Lant Flt
Commander Training Command, Pac Flt
Commander Submarine Development Group TWO
Commander Service Force, Pac Flt, Library
Commander Service Force, Lant Flt
Anti-Submarine Defense Force, Pac Flt
Commander Key West Test & Evaluation Det.
Air Development Squadron ONE (VX-1)
Fleet Sonar School
Fleet ASW School, San Diego
Beach Jumper Unit ONE
Beach Jumper Unit TWO
Naval Air Development Center, Library
Naval Missile Center, Technical Library, Code 5320
Naval Air Test Center (NANEP)
Naval Ordnance Laboratory, Library (2)
Naval Ordnance Test Station, Pasadena Annex Library
Naval Ordnance Test Station, China Lake
  Code 753 Technical Director
David Taylor Model Basin, Library
Naval Engineering Experiment Station Library
Navy Mine Defense Laboratory, Code 712
Naval Training Device Center
Naval Underwater Ordnance Station
Office of Naval Research, Pasadena
Naval Medical Research Laboratory
Naval Personnel Research Field Activity. Washington, D. C.
Navy Hydrographic Office, Library
  Oceanography Division
Navy Underwater Sound Laboratory
  Code 1450 (3)
  Harold Nash Stanley Peterson
  (Secret) (1)
Lant Fleet, ASW Tactical School
Naval Research Laboratory
  Code 2027 (2) Code 4000
  Code 5400 Code 5120
Navy Underwater Sound Reference Laboratory, Library
Navy Electronics Liaison Office
Naval Postgraduate School
  (Library) (2)
Navy Representative, Project LINCOLN, MIT
Asst. SECNAV, Research & Development
Department of Defense, Director of Def. Res. & Engr. (Tech. Library)
  (Weapons Systems Evaluation Group)
  (Guided Missiles)
Asst. Chief of Staff, G-2, US Army
  (Document Library Branch) (3)
Army Electronic Proving Ground
  (Technical Library)
Redstone Arsenal (Technical Library)
Beach Erosion Board, US Army
Air Defense Command (Office of Operations Analysis)
Air University Library, AUL3T-5028
Air Force Cambridge Research Center
  CRQSL-1
Rome Air Development Center (RCRES-4C)
Holloman Air Force Base (SRLTL)
University of California, Marine Physical Laboratory
University of California, Scripps Institution of Oceanography

VIA BUSHIPS:

National Research Council (Committee on Undersea Warfare, Executive Sec.) (2)
Brown University, Research Analysis Group
Pennsylvania State University, Ordnance Research Laboratory
The University of Texas
  Military Physics Laboratory
  Defense Research Laboratory
University of Washington, Applied Physics Laboratory
Woods Hole Oceanographic Institution
Bell Telephone Laboratories, Murray Hill
Bendix Aviation Corp., North Hollywood
Edo Corp., Long Island
General Electric Co., Syracuse
Raytheon Mfg. Co., Wayland
Sangamo Electric Co., Springfield

VIA ONR New York Branch:

Laboratory of Marine Physics, New Haven
Columbia University, Hudson Laboratories

VIA ONR Boston Branch:

Harvard University, Acoustics Research Laboratory, Dr. F. V. Hunt

VIA ONR RES REP, University of Michigan:

University of Michigan Research Institute